Available online at www.sciencedirect.com
ScienceDirect
Applied Clay Science 40 (2008) 27–37
Applied CLAY Science
www.elsevier.com/locate/clay

Influence of M^{II}/M^{III} ratio in surface-charging behavior of Zn–Al layered double hydroxides

R. Rojas Delgado [a,1], C.P. De Pauli [a,*], C. Barriga Carrasco [b,2], M.J. Avena [c,3]

[a] *INFQC, Departamento de Fisicoquímica, Facultad de Ciencias Químicas, Universidad Nacional de Córdoba, Ciudad Universitaria, 5000 Córdoba, Argentina*

[b] *Departamento de Química Inorgánica e Ingeniería Química, Campus de Rabanales, Universidad de Córdoba, Edificio C-3, 14071, Córdoba, Spain*

[c] *Departamento de Química, Universidad Nacional del Sur, Avenida Alem 1253, 8000 Bahía Blanca, Argentina*

Received 31 January 2007; received in revised form 20 June 2007; accepted 22 June 2007
Available online 10 July 2007

Abstract

Zn–Al layered double hydroxides with different M^{II}/M^{III} ratios were synthesized by the coprecipitation method and the obtained solids were characterized by powder X-ray diffraction, infrared spectroscopy, acid–base potentiometric titrations, electrophoretic mobility and modeling of the electrical double layer. As general behavior, increasing hydroxyl adsorption with increasing pH and decreasing supporting electrolyte concentration takes place between pH 7 and 12. The electrophoretic mobility of the samples are in all cases positive and it decreases when the pH becomes higher than 9. A net positive charge of the particles, with a point of zero charge (PZC) around 11.8, is deduced from electrophoretic data. A modified MUSIC model, where OH^-/Cl^- exchange at structural sites and proton desorption from surface hydroxyl groups are taken into account, is used to estimate the deprotonation constants, the number of surface groups, the number of sites with structural charges an the affinity constants for Cl^- and OH^- of the samples with different M^{II}/M^{III} ratios. The modeling of potentiometric titrations and electrophoresis data indicates that anions between the layers and negatively charged groups in the particle surface balance most of the structural charge at the particles surface. It shows an important variation of the number of structural sites with the M^{II}/M^{III} ratio and an important role of surface protonation–deprotonation sites to the electrical behavior and exchange properties of LDHs.

Keywords: Layered double hydroxides; Acid–base potentiometric titrations; Electrophoretic mobilities; Electric double layer

1. Introduction

Layered solids with intercalation properties cover a wide variety of materials with important applications as catalysts, exchangers, adsorbents, etc. These materials can be classified by the charge excess in the layers of the host material (Wells, 1984) into three groups: solids with neutral layers, such as graphite; solids with negatively charged layers, such as phyllosilicate clays (Sposito, 1984) and solids with positively charged layers, represented by layered double hydroxides (LDHs) or hydrotalcites (Bruce and O'Hare, 1997; Newman and Jones, 1999; Rives, 2001).

In solid phase the positively charged layers of LDHs are balanced by anions, which can be inorganic (from

* Corresponding author. Fax: +54 351 4334188.
E-mail addresses: rrojas@mail.fcq.unc.edu.ar (R. Rojas Delgado), depauli@mail.fcq.unc.edu.ar (C.P. De Pauli), iq1bacac@uco.es (C.B. Carrasco), mavena@uns.edu.ar (M.J. Avena).
[1] Fax: +54 351 4334188.
[2] Fax: +34 957 418 648.
[3] Fax: +54 291 4595160.

0169-1317/$ - see front matter © 2007 Elsevier B.V. All rights reserved.
doi:10.1016/j.clay.2007.06.010

chloride or nitrate (Khan and O'Hare, 2002) to polioxometalates (Ulibarri et al., 1994)), coordination compounds (Rives and Ulibarri, 1999), organic anions (Carlino, 1997) or even biomolecules (Choy et al., 2000). Thus, interlayer ions are responsible for the solid electroneutrality in solid phase, but when immersed in aqueous solutions some of the interlayer anions move to the aqueous solution and the solid develops an electric double layer at the surface, allowing exchange with ions from the solution.

Not only electrostatic forces (which rule ion exchange) are involved in the processes that take place when layered solids are immersed in an aqueous solution. The surface of these solids may establish chemical bonds (sometimes called specific bonds) with species in the aqueous phase. For example, the proton and ion binding properties of groups located at the edges of phyllosilicate layers are especially reactive (Baeyens and Bradbury, 1999; Avena, 2002). The charging behavior of phyllosilicate particles can be theoretically described by assuming that the particles carry two kind of electrical charges: "permanent" structural charges, that are the main responsible for the cation exchange properties and "variable" (pH dependent) charges resulting from proton adsorption–desorption reactions at the edge groups. Whereas the structural charge is negative, the variable charge can be positive, neutral or negative depending of the degree of protonation of the edge surface. Since the amount of edge groups is usually lower than the amount of permanent charges these solids carry a net negative charge. Recent theoretical studies have succeeded in explaining proton adsorption–desorption processes, electrokinetic data, ion (others than proton) adsorption measurements and electrical double layer properties of phyllosilicates (Kraepiel et al., 1998; Avena and De Pauli, 1998).

The charging and binding properties of surface groups of LDHs were poorly studied, although some reports about chemical bonds with protons and ions exist in the literature (How et al., 2001; Li et al. 2003). In a previous work (Rojas Delgado et al., 2004) a model assuming the presence of these two types of charges in a Zn–Cr LDH was used and the charging behavior of this solid was successfully explained. In contrast to the behavior observed with phyllosilicates, the development of charges at variable charge groups in LDHs seems to be important enough to produce a significant decrease in the zeta potential and to reach a PZC at high pH values.

The crystal structure of LDHs is based on a stacking of brucite-like layers where a fraction x of divalent cations is substituted by trivalent cations (De Roy et al., 1992). The general formula of these compounds is $\left[M^{II}_{1-x}M^{III}_{x}\cdot(OH)_2\right]A^{n-}_{x/n}\cdot mH_2O$, where M^{II}, M^{III} and A^{n-} represent the divalent cation, the trivalent cation and the anion that neutralizes the positive structural charge, respectively. One positive charge per substituting trivalent cation is introduced in the structure, so M^{II}/M^{III} will affect the exchange capabilities of the intercalation compounds and will determine their surface-charging behavior.

In this work we study the influence of M^{II}/M^{III} ratio in the charging properties of LDHs. With this aim we studied the proton adsorption and electrokinetic behavior of Zn–Al LDHs with different Zn^{2+}/Al^{3+} ratios at different pHs and electrolyte concentrations. A model including anionic exchange and protonation–deprotonation processes at the surface of the particle was applied to these data in order to explain them.

2. Experimental

2.1. Samples preparation

The samples were prepared by coprecipitation at controlled pH (Cavani et al., 1991), as described previously for Zn and Al containing LDHs (Badreddine et al., 1998; Ennadi et al., 2000). 200 ml-mixtures of $ZnCl_2$ and $AlCl_3$ (both Anedra) aqueous solutions, with different $[Zn^{2+}]/[Al^{3+}]=R=2.4$, 3.6 and 4.8 ratios and the same $[Zn^{2+}]+[Al^{3+}]=0.1$ M were added drop wise in a flask containing a vigorously stirred 0.1 M NaCl (Merck) solution. The reaction pH was set constant to 7 by the simultaneous addition of a KOH solution. Once the addition of reactants was finished, the resulting slurry was left under stirring for 72 h. The precipitate was then separated from the supernatant by centrifugation and then washed several times with water. The wet solid obtained was dispersed in water and kept at pH 7 as a stock suspension until it was used. The samples will be named ZnAl2, ZnAl3, ZnAl4 according to the different $[Zn^{2+}]/[Al^{3+}]=R$ ratio in the starting solutions.

All solutions were prepared with purified water (Milli-Q system) boiled and purged with N_2. All samples were prepared at room temperature and under a stream of N_2 in order to avoid, or at least minimize, the contamination by atmospheric CO_2.

2.2. Experimental techniques

2.2.1. Structural characterization

Elemental chemical analysis was carried out in an AA-3100 instrument from Perkin Elmer; samples were dissolved in minimum necessary volume of HCl 35% (w/w) and then diluted to the appropriate concentration. To obtain the water content of the LDHs samples, an aliquot of the stock suspension was centrifuged and dried at 70 °C, weighted and then heated at 150 °C to quantify the weight loss between both temperatures. Powder X-Ray diffraction (PXRD) patterns of a previously dried sample were recorded in a Rigaku Miniflex instrument, using a Cu-kα ($\lambda=1.5418$ Å). FT-IR spectra were recorded following the KBr pellet technique (1% weight sample in KBr) in a FT-IR Bruker IFS28 instrument.

2.2.2. Surface studies

In order to measure the proton adsorption–desorption of LDHs, series of acid–base potentiometric titrations at different salt concentrations were performed for every LDH sample. The method is similar to that used for metal oxides and clay minerals (Avena, 2002) and for LDHs in a previous work (Rojas Delgado et al., 2004). A 60 ml dispersion containing 1 g of the corresponding LDH was prepared by diluting the stock dispersion with a NaCl solution of the desired concentration. The suspension was allowed to equilibrate for 1 hour under stirring and N_2 bubbling, and then titrated with a standard KOH solution. The titrant volume added was set in every addition to achieve a pH variation lower than 0.2 units. After each titrant addition, the slurry was stirred until equilibration, the readings being accepted when the drift was less than 0.2 mV/min. The titration was stopped when the pH was around 12, and then, to check reversibility, the same suspension was back-titrated with a standard HCl solution. No data could be obtained at higher pH values because of the extremely high buffer capacity of aqueous solutions under these conditions, which results in unreliable blank corrections.

The proton and hydroxyl adsorption were calculated as the difference between total amounts of H^+ or OH^- added to the dispersion and those required to bring a blank solution of the same volume and electrolyte concentration to the same pH. This procedure was performed for all samples studied at three different NaCl concentrations. The measurements were done at a constant temperature (30 °C) and with N_2 bubbling to avoid CO_2 contamination.

Electrophoretic mobilities were measured using a Rank Brothers electrophoresis apparatus, equipped with a 2 mm-cylindrical cell. An aliquot of the corresponding stock suspension was added to 200 ml of a 0.01 M NaCl solution and was ultrasonically dispersed. The pH of this dispersion was decreased to approximately 6 with an HCl solution and afterwards increased adding NaOH until pH = 11.5 in 0.5–1 pH-units steps. In every step the suspension was stirred for 5 min and the pH and μ were then measured. All dispersions were prepared and used in a N_2 atmosphere to avoid contamination with carbon dioxide. Electrophoretic mobilities were converted to zeta potentials (ζ) with the Smoluchowski equation in order to use these data in the surface-charging model, but it must be considered that ζ values obtained by this equation are only estimations as it can present deviations at high ionic strength for this kind of particles.

In all cases, titrants additions were done with a 665 Dosimat (Metrohm) automatic dispenser and pH was measured with an Orion EA 940 pH meter equipped with an Orion BN 9101 glass electrode and an Orion 900200 double junction Ag/AgCl/Cl reference electrode.

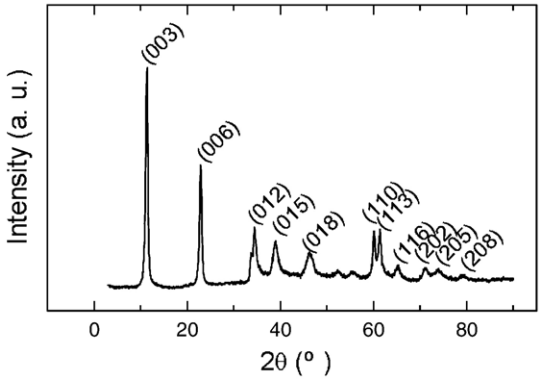

Fig. 1. PXRD diagram of ZnAl2 sample.

3. Results

3.1. Structural characterization

The chemical compositions of the different LDHs are included in Table 1, which shows that the $[Zn^{2+}]/[Al^{3+}]$ ratio in the solids is close to that in the starting solutions. The formula in the table considers that chloride is the only compensating anion and does not take into account the possible presence of carbonate impurities in the interlayer space.

The PXRD patterns were quite similar for the three compounds prepared. Fig. 1 shows the pattern for the sample ZnAl2, as an example. The patterns were indexed in a rhombohedral lattice and reveal the layered structure of these solids. The cell parameters of the three samples are included in Table 2. The c parameter (which represents the thickness of three layers plus the interlayer space between them) was calculated from the average of (00l) reflections. The c parameter decreases as the M^{II}/M^{III} ratio decreases, what has been assigned (Rives, 2001) to stronger interactions between the layers and the interlayer anions. The a dimension (which represents the shortest distance between two cations of the layer) was calculated as twice the position of the (110) reflections. This parameter decreases as the Al^{3+} content increases, as

Table 1
Elemental chemical analysis data and interlayer water content of Zn,Al-LDH samples and their calculated formulae

Sample	M^{II}/M^{III}_{teor}	% Zn	% Al	M^{II}/M^{III}_{exp}	% H_2O	Chemical formulae
ZnAl2	2.4	43.0	7.7	2.3	6.8	$Zn_{0.70}Al_{0.30}(OH)_2Cl_{0.3}\cdot 0.4H_2O$
ZnAl3	3.6	48.0	5.6	3.5	6.5	$Zn_{0.78}Al_{0.22}(OH)_2\cdot Cl_{0.22}\cdot 0.38H_2O$
ZnAl4	4.8	50.7	4.3	4.9	7.1	$Zn_{0.83}Al_{0.17}(OH)_2\cdot Cl_{0.17}\cdot 0.42H_2O$

Table 2
Crystallographic parameters, molecular weight, total layer specific area and calculated density of structural charges of Zn,Al-LDH samples

Sample	a(Å)	c(Å)	M(g)	S(m^2/g)	FN_{str} (C/m^2)
ZnAl2	3.06	22.8	105.7	924	0.30
ZnAl3	3.08	23.2	105.6	936	0.21
ZnAl4	3.10	23.3	106.5	941	0.16

observed in other LDHs (López-Salinas et al., 1997), because this cation has a lower ionic radius than Zn^{2+}.

Table 2 contains values of total layer specific area, S, calculated (S. P. Li et al., 2003) from lattice parameters and chemical composition with the equation $S=3^{1/2}a^2N/M$ where a is the lattice parameter, N is the Avogadro's constant and M is the chemical formula weight. The total specific area of the layers of all samples is similar. N_2 adsorption was not used to measure the specific surface area because in layered solids as phyllosilicate and LDHs N_2 cannot enter the interlayer space, so it cannot give a measure of the total area of the layers.

The FT-IR spectra of the three Zn–Al–Cl LDH samples were also similar. The spectrum of ZnAl2 is given in Fig. 2 as an example. They present a very intense band around 3440 cm^{-1}, which is due to the stretching vibration of hydroxyl groups of the sheets and water molecules of the interlayer domain. The deformation vibration of water molecules is responsible for the broad band recorded at 1618 cm^{-1}. Lattice vibrations appear in the 414–613 cm^{-1} range. The weak band at 1354 cm^{-1} indicates the presence of small amounts of carbonate in the galleries. The spectra agree with the more exhaustive description given by Kloprogge et al. (2004).

3.2. Surface studies

Potentiometric titration data for Zn–Al LDHs samples are shown in Fig. 3a, b and c as hydroxyl consumption (σ_{OH}) vs pH curves. Symbols represent experimental data and lines represent model predictions (see Modeling section). Titration data include points obtained by titration from low pH to high pH with a KOH solution together with points obtained by titration from high pH to low pH with a HCl solution. The coincidence of data for a given NaCl concentration indicates good reversibility in the titration curves. Fig. 3 shows that all samples have a net OH^- consumption in the pH range measured. OH^- consumption starts at around pH = 7 and increases as pH increases. It can be also observed that at a given pH an increase in the electrolyte concentration produces a decrease in OH^- consumption. The greatest separation of the curves at different electrolyte concentration is obtained at pH around 11 and at higher pH values the curves approach each other.

Zeta potential vs. pH curves are also shown in Fig. 3. All samples show a positive ζ in the studied pH range, although the decrease of ζ as the pH increases suggests that the isoelectric point should be at pH 12 or somewhat higher. However, no reliable measurements could be performed at these high pH values because of the increase of the ionic strength under these conditions.

The general behavior presented in Fig. 3 was previously observed for a Zn–Cr LDH (Rojas Delgado et al., 2004). Besides this general behavior, some interesting differences can be found comparing the data of the three samples studied here. The maximum hydroxyl adsorption increases with increasing M^{II}/M^{III} ratio in the samples, from almost 0.15 C/m^2 for ZnAl4 to around 0.30 C/m^2 for ZnAl2, which can be related to the larger anion exchange capacity of the sample with higher Al^{3+} content. On the other hand, ζ vs. pH curves show little variation when structural charge is varied, indicating that zeta potentials and isoelectric points are rather independent on the density of structural charges.

4. Discussion

The crystal structure of LDHs is based on $M(OH)_6$ octahedral units sharing edges, building a sequence of brucite-like layers where isomorphic substitution of a fraction x of divalent cations by trivalent cations occurs. The layers become therefore charged, as one positive charge per substituting trivalent cation is introduced into the structure. Therefore, the structural charge density results to be proportional to the trivalent metal ratio $x=M^{III}/(M^{II}+M^{III})$. In the case of Zn–Al LDHs $Zn(OH)_6$ and $Al(OH)_6$ octahedra are arranged in the layers on a hexagonal structure of parameter a_0. For particular values

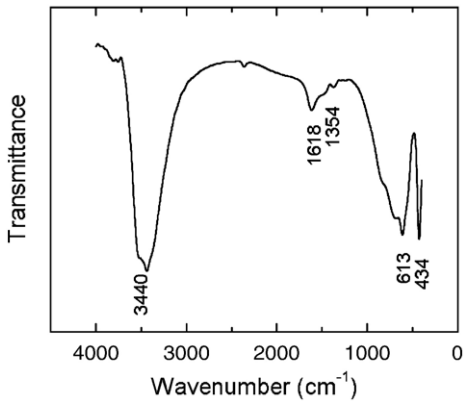

Fig. 2. FT-IR spectra of ZnAl2 sample.

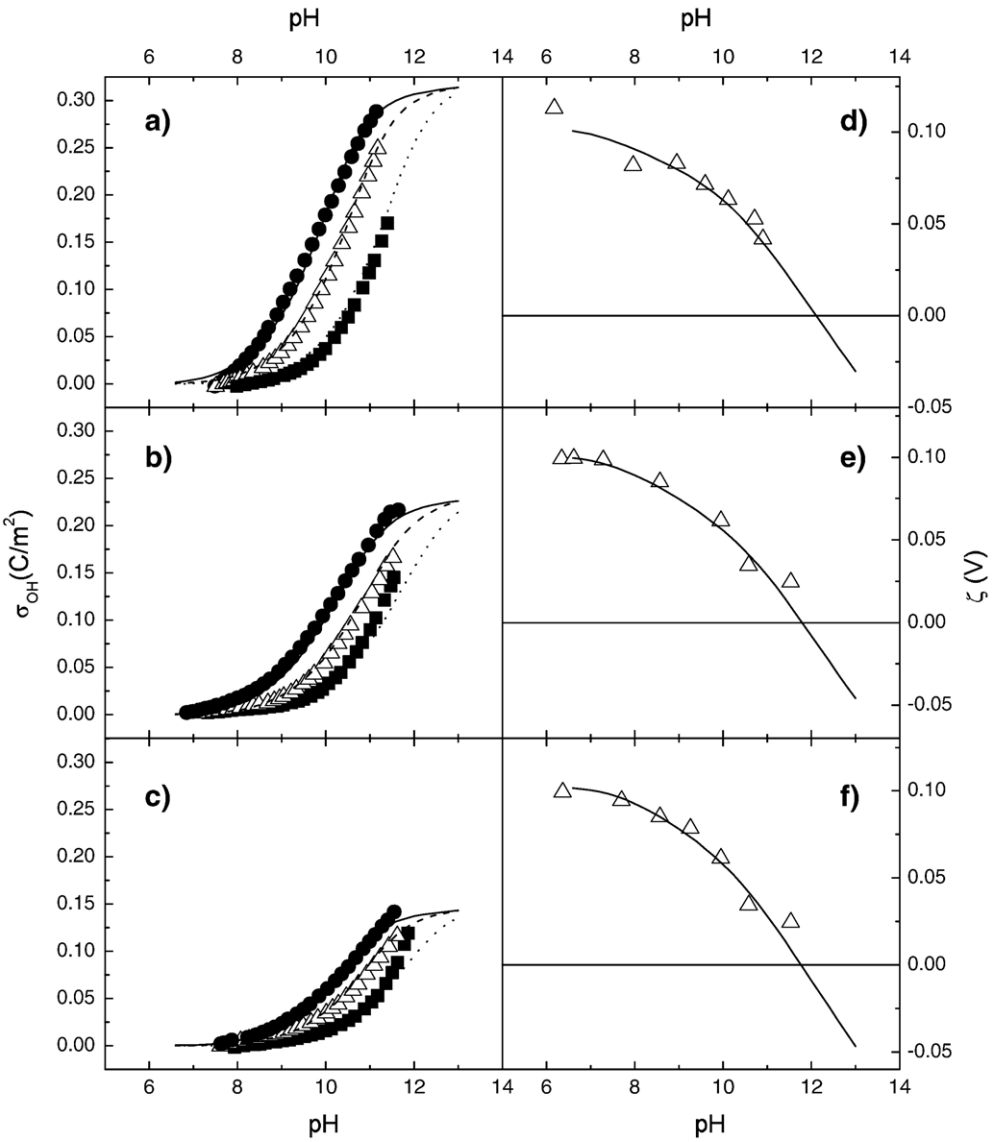

Fig. 3. Experimental (symbols) and calculated (lines) σ_{OH} vs. pH and ζ vs pH curves. Circles and solid lines: 0.01 M NaCl; triangles and dashed lines: 0.1 M NaCl; 1 M NaCl. (a and b) ZnAl2 sample; (c and d) ZnAl3 sample; (e and f) ZnAl4 sample. The ionic strength in the calculations was obtained from NaCl concentrations using the Davies equation.

of x, ordering of divalent and trivalent cations can form superstructures, although the existence of such superstructures has been demonstrated in only a few cases.

LDHs can be synthesized with M^{II}/M^{III} ratios varying from 2 to 4 and even more. The upper limit is generally attributed to electrostatic repulsion between adjacent trivalent metals in the layers. Too high values of M^{II}/M^{III} would result in collapse of the interlamellar domain as they are less populated by charge compensating anions. For Zn–Al-LDHs it has been described that at neutral pH, LDH phases can be obtained with M^{II}/M^{III} varying from 5 to 1.

In this work, integer values of this relation have been avoided in order to stay away from superstructures, so we can suppose a random distribution of the metallic cations in the layers. Since neither of the samples has superstructures it can be supposed that all of them have a similar layer structure. Differences can be found between the LDHs when the composition of their interlayer space is considered. Depending on the synthesis conditions and the Zn/Al ratio they can differ in the water content and/or the type and concentration of exchangeable anions that neutralize the positive charge. It is well known that chloride is easily exchanged by

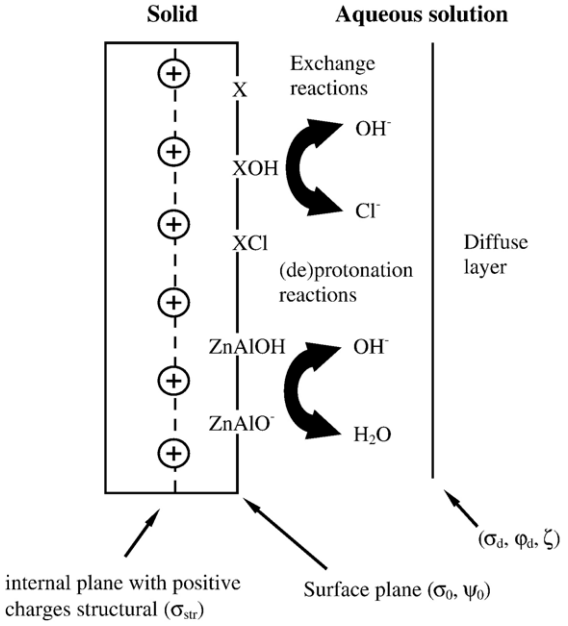

Fig. 4. Schematic drawing of the LDH/solution interface according to the proposed model.

other anions when dispersed in aqueous solution. Carbonate anions, on the contrary, are strongly attached to brucite-like layers and they only can be exchanged at very low pHs (Ulibarri et al., 1995). Then, avoiding the presence of carbonate anions during synthesis and characterization is a fundamental issue to study the surface-charging behavior of LDHs.

PXRD and FT_IR data in Figs. 1 and 2 are typical of LDHs and similar to the reported in the literature for pure chloride intercalated Zn–Al-LDHs phases (Badreddine et al., 1998; Legrouri et al. 2005). These facts, together with the chemical analyses and water content measurements, allow us to propose chemical formulae for the prepared samples (Table 1). It has been considered that the interlayer space is occupied only by chloride anions, which where present at relatively high concentration during the synthesis of the solids.

Fig. 3 shows that LDHs consume a considerable quantity of hydroxyl anions as pH is increased. OH^- consumption by Zn–Al-LDHs will be considered to take place by two mechanisms: one of them is anionic exchange of chloride anions in the interlayer by hydroxyl anions of the solution. This process can be written as:

$$XCl^- + OH^- = XOH^- + Cl^- \quad (1)$$

where X represents groups located in the surface, capable of attaching Cl^- or OH^- anions, forming XCl^- and XOH^- groups. OH^- and Cl^- represents in the equation the anionic species in the solution bulk. It is a simplification of the actual procedure of structural charge balancing as balancing anions are situated in the particle surface as well as in the bulk of the solid, placed between the layers. Anyway, the process clearly indicates that increasing the pH value or decreasing the chloride anion concentration increases OH^- consumption. This agrees, at least qualitatively, with trends shown in Fig. 3.

The other OH^- consuming process is given by the reactivity of surface hydroxyls attached to metal ions in the layers. In Zn–Al-LDHs, hydroxyls are bonded to three cations of the same layer, so we can find two types of surface hydroxyl groups: OH^- attached to two Zn^{2+} and one Al^{3+} cations (Zn_2AlOH groups) and others linked only to Zn^{2+} cations (Zn_3OH groups). Hydroxyl groups linked to more than one Al^{3+} cations would be forbidden by the electrical repulsions between adjacent Al^{3+} cations. If these hydroxyls are in contact with the aqueous solution, their constituting oxygen atoms are potentially reactive and can be protonated or deprotonated. The OH^- consumption by the groups can be written in a general formula as

$$SOH + OH^- = SO^- + H_2O \quad (2)$$

where SOH and SO^- represents protonated and deprotonated surface groups (Zn_3OH or Zn_2AlOH groups). As pH increases this reaction will be favored, increasing OH^- consumption as shown in Fig. 3.

4.1. Modeling

According to the two reactions proposed above, the overall OH^- consumption results from two processes: Cl^-/OH^- anionic exchange (Eq. (1)) and deprotonation of surface hydroxyl groups (Eq. (2)). A model of the LDHs-water interface can separate the contribution of both processes. In a previous work we have found that both processes are equally important in order to explain the surface-charging behavior of LDHs, here we will study the effect of M^{II}/M^{III} ratio in both anionic exchange and protonation–deprotonation of surface hydroxyl groups.

The proposed model can be divided into two parts: one representing the surface of the LDH particle, the type and properties of surface sites, the charge distribution in the particle, etc., and other representing the electrical double layer (EDL) that describes the charge distribution and potential decay on the aqueous side of the interface.

The scheme of a LDH layer particle according to the proposed model is shown in Fig. 4. Structural charges are assumed to be internal and placed parallel to the surface of the particle. The charge density in this plane is designated as σ_{str} (C/m^2) and the density of structural charges (mol/m^2) in the internal plane as N_{str}. The relation between them is

$$\sigma_{str} = FN_{str} \tag{3}$$

Although the exchange sites are placed in the surface and also in the bulk of the particle, in this model they are considered to express as discrete sites X that can bind and exchange the anions of the aqueous solution (Cl^- and OH^-), thus compensating the positive charge excess of the particle. In other words, N_{str} will have three components: N_X, N_{XCl} and N_{XOH}, that stand for the density of unscreened charges and of those balanced by chloride and hydroxyl anions, respectively.

The adsorption reactions of Cl^- and OH^- on X sites can be written as follows

$$X + Cl^- = XCl^- \tag{4}$$

$$X + OH^- = XOH^- \tag{5}$$

The intrinsic constants for these processes are

$$K_{Cl}^{int} = \frac{\Gamma_{XCl}}{\Gamma_X[Cl^-]}\exp(-F\psi_0/RT) \tag{6}$$

$$K_{OH}^{int} = \frac{\Gamma_{XOH}}{\Gamma_X[OH^-]}\exp(-F\psi_0/RT) \tag{7}$$

where Γ_{XCl} and Γ_{XOH} denote the surface densities (mol/m^2) of XCl^- and XOH^-, respectively. Γ_{XCl} and Γ_{XOH} represent the positive structural charges canceled by the interlayer anions and Γ_X represents the non-screened structural charges. [Cl^-] and [OH^-] are the activities of the anion in the solution bulk.

The surface also presents SOH groups, which can produce hydroxyl consumption according to Eq. (2), producing also the compensation of a portion of the structural charge. This reaction is equivalent to the deprotonation process

$$SOH = SO^- + H^+ \tag{8}$$

which has the intrinsic deprotonation constant:

$$K_a^{int} = \frac{1}{K_H^{int}} = \frac{\Gamma_{SO}[H^+]}{\Gamma_{SOH}}\exp(-F\psi_0/RT) \tag{9}$$

where K_a^{int} is the intrinsic deprotonation constant of SOH. K_H^{int} is the intrinsic constant of the reverse reaction (protonation of SO^- groups), Γ_{SOH} and Γ_{SO} are the surfaces densities (mol/m^2) of SOH and SO^- groups, respectively, ψ_0 is the potential at the surface of the particle and F, R and T have their usual meaning. The surface density of protonation–deprotonation groups will be denoted N_v ($N_v = \Gamma_{SOH} + \Gamma_{SO}$).

It must be noted that close to the SOH groups exists an excess of positive charge due to the presence of Al^{3+}. The positive charge is not explicitly written in the groups as it is considered as a structural charge forming part of the lattice. The presence of structural charges in the surrounding area of the group may increase the affinity for deprotonation of surface groups because H^+ is repelled by the positive structural charges. In Zn_3OH groups we will suppose that the existence of Al^{3+} cations in the lattice does not affect the reactivity of the group, as it is not directly coordinated to the central OH^-, so these groups will have less affinity for deprotonation than Zn_2AlOH ones, as will be discussed later.

The charge density and the electric potential at the surface plane are denoted as σ_0 and ψ_0, respectively. The charge density at the surface plane can be calculated from the densities of charged sites at this plane; thus

$$\sigma_0 = F(-\Gamma_{XCl} - \Gamma_{XOH} - \Gamma_{SO}) \tag{10}$$

It must be considered that the net charge of the particle will be given by the sum of positive structural charges inside the particle and the negative surface charges, so

$$\sigma_{str} + \sigma_0 = F(\Gamma_X - \Gamma_{SO}) \tag{11}$$

which means that the net charge of the particle results from the non-screened X sites minus the deprotonated surface sites.

The net OH^- consumption (σ_{OH}), as previously said is a combination of hydroxyl used by exchange and deprotonation processes. It can be expressed as

$$\sigma_{OH} = F(\Gamma_{XOH} + \Gamma_{SO}) \tag{12}$$

This model of the solid particle must be combined with an electrostatic one in order to describe charge distribution and potential drop across the solid–liquid interface. The Stern–Gouy–Chapman model is used

Table 3
Refined parameters of the proposed model for Zn,Al-LDH samples

Sample	pK_a^{int}	pK_{Cl}^{int}	pK_{OH}^{int}	FN_v (C/m^2)	FN_{str} (C/m^2)	C (F/m^2)
ZnAl2	12.05	0.20	−1.83	0.28	0.30	0.08
ZnAl3	11.80	−0.15	−1.67	0.25	0.20	0.07
ZnAl4	11.85	−0.44	−1.85	0.22	0.14	0.08

here, which assumes that the surface plane and the diffuse layer are separated by a region of constant capacitance called the Stern layer and that the potential drop across the diffuse layer is described by the Gouy–Chapman equation. The set of equations, confirming this electrostatic model are

$$\psi_0 - \psi_d = (\sigma_{str} + \sigma_0)/C \quad (13)$$

$$\sigma_d = -0.1174 I^{1/2} \sinh(F\psi_d/2RT) \quad (14)$$

$$\sigma_{str} + \sigma_0 + \sigma_d = 0 \quad (15)$$

where σ_d and ψ_d are the charge and the potential in the diffuse layer and I is the ionic strength in the solution, calculated with the Davies equation.

In this model we have proposed only one type of reactive surface group for protonation–deprotonation. This is the classical treatment of the metal (hydr)oxide surface, but it can result physically unrealistic because there is often more than one surface reactive group in real samples (Parks, 1990). To overcome this limitation Hiemstra et al (1989) have developed a method to estimate the intrinsic protonation constant of surface groups of metal oxides and hydroxides. This method has evolved into the termed MUSIC model (Bleam, 1993; Hiemstra et al., 1996), that has been applied to explain, describe and predict the surface behavior of iron, titanium, and other metal oxides as well as phyllosilicate clays (Avena, 2002). The modified MUSIC model relates the affinity of surface groups for protons to the Lewis basicity of surface oxygen atoms, which are the surface groups capable of protonation–deprotonation reactions. It states that bonds with the nearest atoms neutralize the valence V of an oxygen atom in the particle bulk. Each surrounding atom will neutralize part of V with their bond valence (s), estimated as $s = z/\mathrm{CN}$, where z is the valence and CN is the coordination number of the corresponding adjacent atom. At the surface, part of the bonds with the surrounding cations will be broken and new bonds will be formed with hydrogen cations and water molecules. This usually leads to overcompensation or undercompensation of the valence V of surface oxygen, which will react to return to an exact compensation of his valence. Mathematically, it can be written as:

$$\log K_H^{int} = -19.8\left(\sum s_j + V\right) \quad (16)$$

where the parameter −19.8 results from the calibration of the model with the experimental protonation constant of several oxo- and hydroxo-metal complexes in solution (Hiemstra et al., 1996), and Σs_j gives the neutralization of the oxygen valence ($V = -2$) produced by bonds with lattice cations, or protons and water molecules from solution.

In the case of Zn–Al-LDH samples we have considered, as previously said, two kinds of surface hydroxyl groups (Zn_2AlOH and Zn_3OH): the Σs_j will be affected by the presence or absence of Al^{3+} cations in

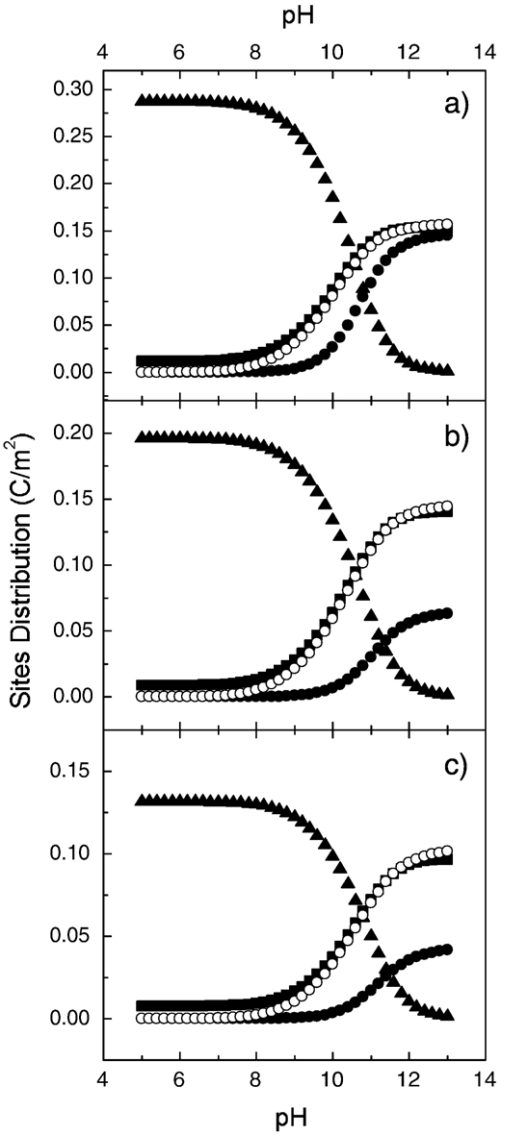

Fig. 5. Model predictions for site distribution at NaCl concentration 0.1 M with parameters of Table 3. Surface sites densities are multiplied by the Faraday constant to obtain C/m^2 units. Triangles, XCl^- groups; solid circles, XOH^- groups; squares, X groups; open circles, Zn_2AlO^- groups. a) ZnAl2 sample; b) ZnAl3 sample; c) ZnAl4 sample.

the surroundings of the oxygen. For Zn_2AlOH and Zn_2AlO^- groups it can be calculated that:

$$\sum s_j = 2s_{Zn} + s_{Al} + ms_H + i(1 - s_H) \quad (17)$$

where s_{Zn} is the bond valence of Zn ($s_{Zn}=2/6$), s_{Al} is the bond valence of Al ($s_{Al}=3/6$), and s_H is the bond valence of a proton donating bond ($s_H=0.8$). The integers m and i denote the number of proton donating and proton accepting hydrogen bonds formed with the surrounding water molecules, and the number 2 indicates that two Zn^{2+} are bonded to the surface oxygen in the group.

In the case of Zn_2AlO^- groups, $m=0$ and i could be either 1 or 2 (there is no information about the exact number of water molecules bounded through hydrogen bond to each surface groups). Calculations with this model assign log K_H^{int} (Zn_2AlO^-)=12.5 for $i=1$ and 8.6 for $i=2$. As we do not know the number of water molecules bonded to the oxygen atom, only a range for the value of log K_H^{int} can be estimated. This suggests that the surface density of Zn_2AlOH and Zn_2AlO^- will vary notably through this pH range: at pH values lower than 8.6 it could be mainly found ZnAlOH groups and at pH values higher than 12.5 principally $ZnAlO^-$ would exist.

A similar estimation can be made for Zn_3OH and Zn_3O^- groups. The absence of Al^{3+} bonded to the oxygen atom will reduce the surface group affinity for deprotonation, as its valence is less oversaturated. It can be calculated that:

$$\sum s_j = 3s_{Zn} + ms_H + i(1 - s_H) \quad (18)$$

For Zn_3O^- groups, i and m can take the same values than for Zn_2AlO^- groups, and the values of K_H^{int} calculated for $i=1$ and 2 are 15.8 and 11.9, respectively. Thus, at pH values below 11.9 these groups will be all protonated and no deprotonation process would be registered. This means that the OH^- consumption registered in the potentiometric titrations shown in Fig. 3 at pH values between 7 and 11 are due mainly to Cl^-/OH^- anionic exchange and surface Zn_2AlOH group deprotonation process.

Other oxygen-containing groups could be located at the surface of Zn–Al LDHs. If the ordering of cations in the layers is not perfect, hydroxyls groups coordinated to two Al^{3+} cations, although in low concentration, could be present. The edge surface may also contain groups different from that of the bulk of the surface, and hydroxyl groups bonded to less than three metallic centers can be found. However, since the thickness of the particles is much lower than their length and width, the edge surface area is very small compared to the basal surface area. Therefore, the number of edge groups will be negligible when compared to the number of basal surface groups and the former will only be important if the latter are nonreactive. This is the case of phyllosilicate clays as montmorillonite and illite, that possess inert SiO_2 groups at the basal surfaces, and ten edge groups control their acid–base behavior (Avena, 2002). However, surface groups at the basal planes are rather reactive in LDHs (Rojas Delgado et al., 2004), and thus reactivity of edges can be ignored.

Although up to six parameters (N_{str}, N_s, K_a^{int}, K_{Cl}^{int}, K_{OH}^{int} and C) must be evaluated in order to solve the equations of the proposed model, some of them can be estimated a priori from structural data or using the modified MUSIC model, and used as initial parameters in a fitting procedure. N_{str}, whose values are shown in Table 2, can be obtained from the total layer specific area and the Al^{3+} content. N_v values can be obtained in a similar way, it can be estimated around 2×10^{-5} mol/m^2 ($F\,N_s=1.9$ C/m^2). This value may not be very accurate because not all the hydroxyl groups in the solid are accessible by the OH^- in solution, being thus nonreactive. The initial value for log K_a^{int} parameter was 10.5, the intermediate value between the calculated with the modified MUSIC model for Zn_2AlOH groups bounded to 1 and 2 water molecules. No values have been found for log K_{Cl}^{int} and log K_{OH}^{int}; therefore their initial values in the fitting procedure have been considered equal to 1, although it seems that LDHs have more affinity for OH^- than for Cl^-(Li et al., 2003). Optimization of the parameter values was performed using the simplex method (Avena and De Pauli, 1998) on the σ_{OH} vs. pH and ζ vs. pH curves, assuming that $\zeta=\psi_d$. This last assumption is usually not valid at relatively high (higher than 0.01 M) electrolyte concentrations because the potential drop in the interface is rather pronounced. This is why we have worked in 0.01 M NaCl for electrophoresis, although we recognize that calculated ψ_d may overestimate somewhat the zeta potentials. In spite of this, calculated ψ_d are compared to ζ just to show that the model predicts the shape of the ζ vs pH curves and the isoelectric points.

The calculated σ_{OH} vs. pH and ζ vs. pH curves for the three prepared samples are shown in Fig. 3, whereas Table 3 list the best-fit parameters for all modeled samples. The model predicts quite well the shape of the curves and their shift with variations of electrolyte concentration and zeta potential data. The best-fit parameters are quite in agreement with the initial estimates in all samples. log K_a^{int} is in the range of 8.5–12.5 calculated by the MUSIC model and values of N_{str} are quite similar to that calculated by structural data. Only

for ZnAl4 sample σ_{str} slightly deviates to lower values, which could be assigned to the carbonate presence in the sample. The parameters also indicate that affinity for OH^- is higher than for Cl^- ($pK_{Cl}^{int} > pK_{OH}^{int}$), as stated previously. The N_v value is quite lower than the initial estimate, as suggested previously, indicating that only 10% of the OH groups are accessible by the solution and thus capable of deprotonation.

As can be seen from optimization values, decreasing M^{II}/M^{III} ratios leads to an increase in N_{str} values. As we have seen before, increasing Al^{3+} content are supposed to produce increasing positive charge excess in the layer, which means an increasing number of exchange sites. On the other hand, N_v value decreases as M^{II}/M^{III} increases because only Zn_2AlOH/ Zn_2AlO^- are considered to be reactive, and their surface concentration is thus proportional to the content of Al^{3+}. pK_a^{int} parameter shows little variation with increasing M^{II}/M^{III} ratio, which seems to support the idea that the same type of protonation–deprotonation surface groups are reacting in all cases. Little variations in K_{Cl}^{int} values also shown in Table 3, but we have found no clear explanation for this.

Fig. 5 shows the predicted LDHs site distribution in 0.1 M electrolyte as a function of pH. The site distribution at other electrolyte concentrations is not shown here but follows similar trends. For all samples studied the model predicts that at pH around 7 the particle surface presents mainly exchange sites attached to chloride anions and protonated Zn_2AlOH groups. It also predicts a small but noticeably density of unoccupied exchange sites, which would be responsible of the positive charge of the particles, resulting in a positive zeta potential. At pH > 7 Zn_2AlOH groups start to consume OH^- from solution and Zn_2AlO^- groups appear. Their surface concentration reaches a plateau at pH above 12. The model predicts that acid–base surface groups are not totally protonated, being the deprotonated groups percentage around 50% for all samples. Above pH = 9 there is also a significant OH^- consumption due to the attachment of hydroxyl anions to exchange sites X, forming XOH^- groups. It is noteworthy that Cl^- anions start to detach from X sites at pH above 7 because of an electrical effect, caused by the presence of deprotonated Zn_2AlO^- groups, that compensates part of the positive structural charge, thus decreasing the surface potential.

The model predicts that most of the positive structural charge of LDHs is screened by XCl^- (at low pHs) or XOH^- and Zn_2AlO^- (at high pH) surface groups. Thus, the net surface charge concentration is very low and even decreases at high pHs, becoming zero at a pH around 11.8. The model also predicts that Zn_2AlOH groups play an important role in electrical surface behavior and anionic exchange properties of LDHs because Zn_2AlO^- negative groups produce screening of structural charge, decreasing the number of exchange sites available and reducing the surface potential, thus decreasing the electrostatic affinity of the surface for chloride anions. As M^{II}/M^{III} increases this effect becomes more important, as the model predicts that the density of exchange sites (N_{str}) decreases more rapidly than protonation–deprotonation sites density (N_v). Thus, at pH = 12 and 0.1 electrolyte concentration, for ZnAl2 sample 46% of X sites is available for exchange, whereas for ZnAl4 sample only 25 % of the sites is available.

5. Conclusions

A model for the reactivity of Zn,Al-LDH surface has been applied in order to explain the hydroxyl adsorption and electrokinetic properties as a function of pH and NaCl concentration and to explain the effects of the sample M^{II}/M^{III} ratio. The adsorption is explained as the sum of two contributions: OH^-/Cl^- anionic exchange because of the presence of structural charges and protonation–deprotonation of surface hydroxyl groups. The reactive oxygen atoms in the surface of LDH particles are bonded to 2 Zn^{2+} cations and one Al^{3+} cations (Zn_2AlOH groups), while oxygen atoms bonded to 3 Zn^{2+} cations are predicted to be non-reactive.

As M^{II}/M^{III} increases the number of structural charges decreases, producing a lower exchange capacity of the solid, and a lower OH^- consumption. On the other hand the lower content of Al^{3+} reduces the number of Zn_2AlOH groups, although the extent of this reduction is lower than for exchange sites.

According to the model the structural charge is compensated at the surface by anions attached to exchange sites and by negatively charged Zn_2AlO^- groups. The remaining non-screened structural charges generate a net positive surface potential in a wide range of pH. Increasing variable charges with increasing pH produces a reduction in the exchange properties of the LDH and finally a reduction in the positive zeta potential, reaching an PZC at pH around 11.8.

The Al^{3+} content reduction increases the variable charges contribution to the electrical behavior of LDHs surface, reducing the LDHs exchange capacity at high pH values.

Acknowledgements

This study was financed by CONICET, SECYT and AECI (PCI program). R. Rojas Delgado thanks AECI (MAE program) and CONICET (post-doctoral grant) for economic support.

References

Avena, M.J., 2002. Acid–base behavior of clay surfaces in aqueous media. In: Hubbard, A. (Ed.), Encyclopedia of surface and colloid science. Marcel Dekker, New York, pp. 17–46.

Avena, M.J., De Pauli, C.P., 1998. Proton adsorption and electrokinetics of an Argentinean montmorillonite. Journal of Colloid and Interface Science 202, 195–204.

Badreddine, M., Barroug, A., Khaldi, M., Legrouri, A., De Roy, A., Besse, J.P., 1998. Chloride-hydrogenophosphate ion exchange into the zinc–aluminium–chloride layered double hydroxide. Materials Chemistry and Physics 52, 235–239.

Baeyens, B., Bradbury, M.H., 1999. A mechanistic description of Ni and Zn sorption on Na-montmorillonite Part I: titration and sorption measurements. Journal of Contaminant Hydrology 27, 199–222.

Bleam, W.F., 1993. On modeling proton affinity at the oxide/water. Journal of Colloid and Interface Science 159, 312–318.

Bruce, D.W., O'Hare, D., 1997. Inorganic Materials. Wiley, Chichester.

Carlino, S., 1997. The intercalation of carboxylic-acids into layered double hydroxides— a critical evaluation and review of the different methods. Solid State Ionics 98, 73–84.

Cavani, F., Trifiro, F., Vaccari, A., 1991. Hydrotalcite-type anionic clay: preparation and application. Catalysis Today 11, 173–301.

Choy, J.-H., Kwak, S.-Y., Jeong, Y.-J., Park, J.-S., 2000. Inorganic layered double hydroxides as nonviral vectors. Angewandte Chemie 11, 1671–1674.

De Roy, A., Forano, C., El Malki, K., Besse, J.P., 1992. Trends in pillaring chemistry. In: Ocelli, M.L., Robson, H.E. (Eds.), Expanded Clays and other Microporous Solids. Van Nostrand Reinhold, New York, pp. 108–169.

Ennadi, A., Legrouri, A., De Roy, A., Besse, J.P., 2000. X-ray diffraction pattern simulation for thermally treated [Zn–Al–Cl] layered double hydroxide. Journal of Solid State Chemistry 152, 568–572.

Hiemstra, T., De Witt, J.C.M., Van Riemsdijk, W.H., 1989. Multisite proton adsorption modeling at the solid/solution interface of (hydr) oxides: a new approach. Journal of Colloid and Interface Science 133, 91–117.

Hiemstra, T., De Witt, J.C.M., Van Riemsdijk, W.H., 1996. Intrinsic proton affinity of reactive surface groups of metal (hydr)oxides: the bond valence principle. Journal of Colloid and Interface Science 184, 680–692.

How, W.-G., Su, Y.-L., Sun, D.-J., Zhang, C.-G., 2001. Studies on zero point of charge and permanent charge density of Mg–Fe hydrotalcite-like compounds. Langmuir 17 (6), 1885–1888.

Khan, A.I., O'Hare, D., 2002. Intercalation chemistry of layered double hydroxides: recent developments and applications. Journal of Materials Chemistry 12, 3191–3198.

Kloprogge, J.T., Frost, R.L., Hickey, L., 2004. FT-Raman and FT-IR spectroscopic study of synthetic Mg/Zn/Al-hydrotalcites. Journal of Raman Spectroscopy 35, 967–974.

Kraepiel, A.M.L., Keller, K., Morel, F.M.M., 1998. On the acid–base chemistry of permanently charged minerals. Environmental Science and Technology 32, 2829–2838.

Legrouri, A., Lakraimi, M., Barroug, A., De Roy, A., Besse, J.P., 2005. Removal of the herbicide 2,4-dichlorophenoxyacetate from water to zinc–aluminium–chloride layered double hydroxides. Water Research 39, 3441–3448.

Li, S.-P., How, W.-G., Han, S.-H., Li, L.-F., Shao, W.-A., 2003. Studies on intrinsic ionization constants of Fe–Al–Mg hydrotalcite-like compounds. Journal of Colloid and Interface Science 257, 244–249.

López-Salinas, E., García-Sánchez, M., Montoya, J.A., Acosta, D.R., Abasolo, J.A., Schifter, I., 1997. Structural characterization of synthetic hydrotalcite-like $[Mg_{1-x}Ga_x(OH)_2](CO_3)_{x/2}\times\cdot mH_2O$. Langmuir 13, 4748–4753.

Newman, S.P., Jones, W., 1999. Comparative study of some layered hydroxide salts containing exchangeable interlayer anions. Journal of Solid State Chemistry 148, 26–40.

Parks, G.A., 1990. Surface energy and adsorption at mineral/water interfaces: an introduction. In: Hochella, M.F., White, A.F. (Eds.), Mineral–Water Interface Geochemistry. Reviews in Mineralogy, vol. 23. Mineralogical Society of America, Washington D. C., pp. 133–175.

Rives, V., 2001. Layered Double Hydroxides: Present and Future. Nova Sci. Pub. Inc., New York.

Rives, V., Ulibarri, M.A., 1999. Layered double hydroxides (LDH) intercalated with metal coordination compounds and oxometalates. Coordination Chemistry Reviews 181, 61–120.

Rojas Delgado, R., Arandigoyen Vidaurre, M., De Pauli, C.P., Ulibarri, M.A., Avena, M.J., 2004. Surface-charging behavior of Zn–Cr layered double hydroxide. Journal of Colloid and Interface Science 280, 431–441.

Sposito, G., 1984. The Surface Chemistry of Soils. Oxford University Press, New York.

Ulibarri, M.A., Labajos, F.M., Rives, V., Trujillano, R., Kagunya, W., Jones, W., 1994. Comparative study of the synthesis and properties of vanadate-exchanged layered double hydroxides. Inorganic Chemistry 33, 2592–2599.

Ulibarri, M.A., Pavlovic, I., Hermosín, M.C., Cornejo, J., 1995. Hydrotalcite-like compounds as potential sorbents of phenols from water. Applied Clay Science 10, 131–145.

Wells, A.F., 1984. Structural Inorganic Chemistry, 5th edition. Oxford Sci. Pub., Oxford.